Supporting Information

Tailoring carboxylatopillar[5]arene modified magnetic graphene oxide nanocomposites for efficient removal of cationic dyes

Yu Huang [†a], Yanqin Rong [†a], Wenjia Zhang [a], Zibin Zhang[*b], Xiaoyuan Zhang [a], Wenting Liang[*a], Cheng Yang [*a, c]

[a] Institute of Environmental Sciences, Department of Chemistry, Shanxi University, Taiyuan, 030006, China. E-mail: liangwt@sxu.edu.cn (W. T. Liang)

[b] College of Material, Chemistry and Chemical Engineering, Key Laboratory of Organosilicon Chemistry and Material Technology, Ministry of Education, Key Laboratory of Organosilicon Material Technology, Hangzhou Normal University, Hangzhou 311121, China. Email: zzhang@hznu.edu.cn (Z. Zhang)

[c] Key Laboratory of Green Chemistry & Technology of Ministry of Education, Sichuan University, Chengdu 610064, China. E-mail: yangchengyc@scu.edu.cn (C. Yang)

[†] The authors contributed equally: Yu Huang, Yanqin Rong

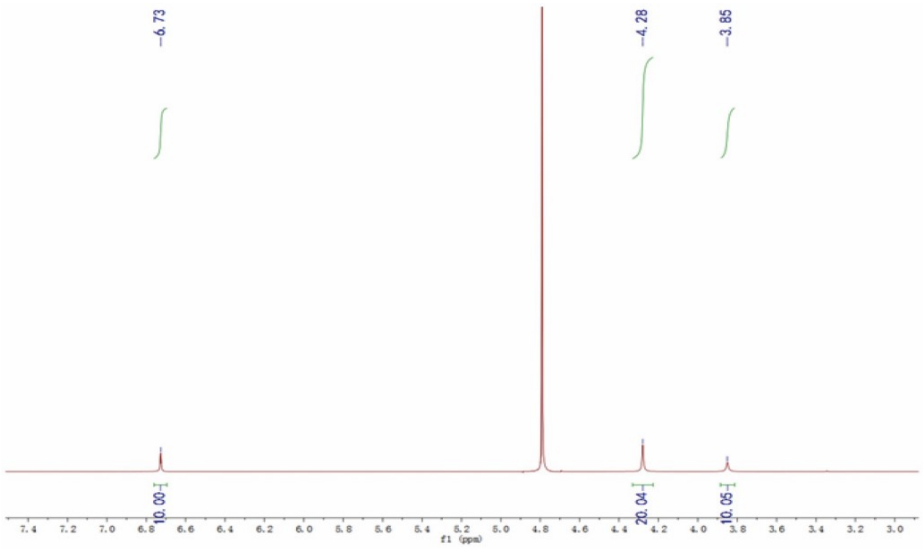

Fig. S1 ^{1}H NMR spectrum of carboxylatopillar[5]arene. ^{1}H NMR (500 MHz, D_2O) δ 6.67 (s, 10H), 4.26 (s, 20H), 3.78 (s, 10H).

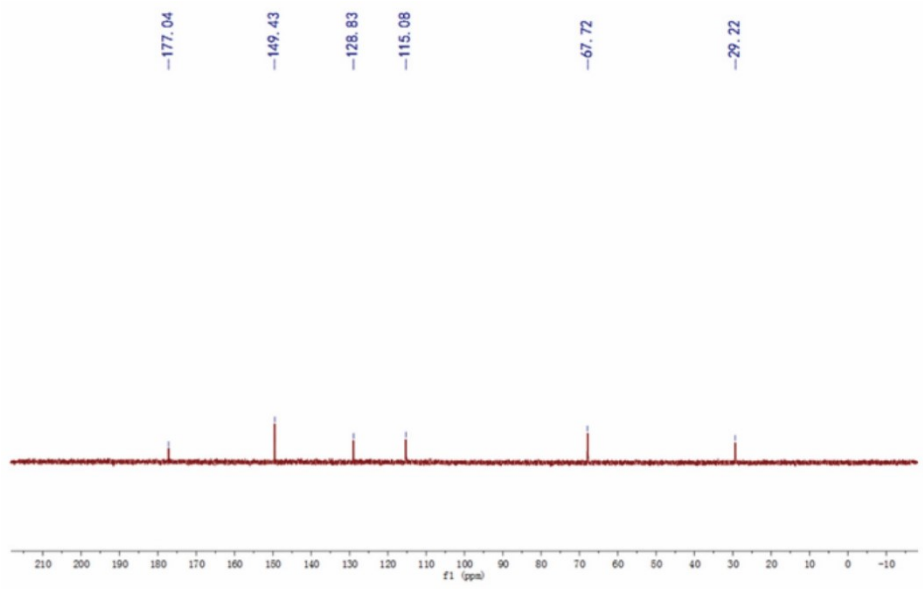

Fig. S2 ^{13}C NMR spectrum of carboxylatopillar[5]arene. ^{13}C NMR (126 MHz, D_2O) δ 177.04 (s), 149.43 (s), 128.83 (s), 115.08 (s), 67.72 (s), 29.37 (s).

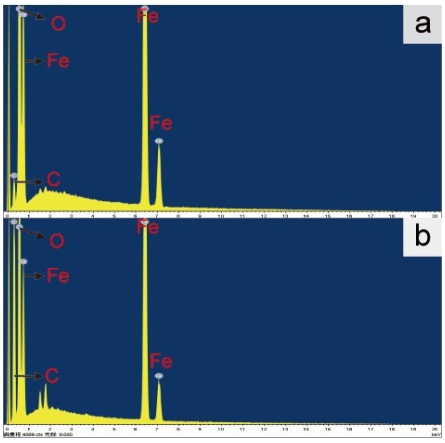

Fig. S3 The EDS analysis of MGO (a) and MGO@CP5 (b).

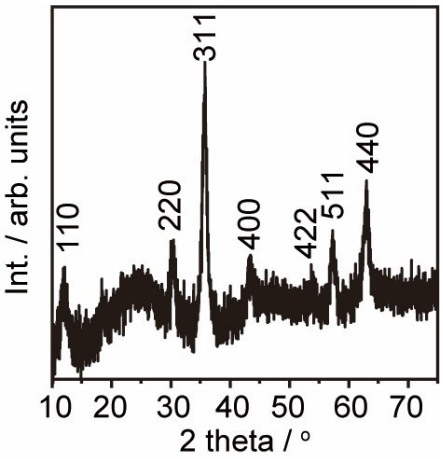

Fig. S4 XRD pattern of MGO@CP5.

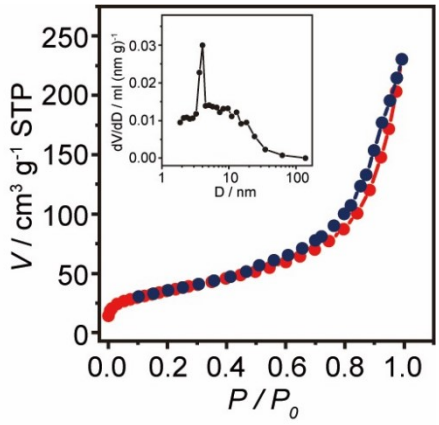

Fig. S5 N_2 adsorption / desorption isotherms of MGO@CP5. Insert: the pore size distribution curve of MGO@CP5.

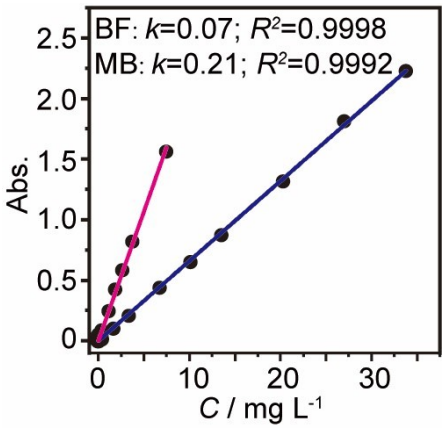

Fig. S6 The standard curves of BF and MB solution.

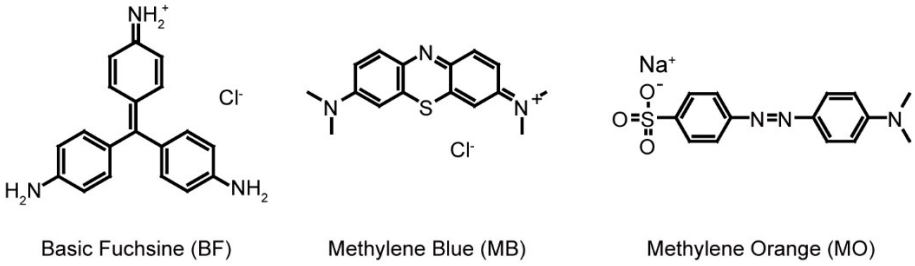

Fig. S7 The structure of cationic dye (BF and MB) and anionic dye (MO).

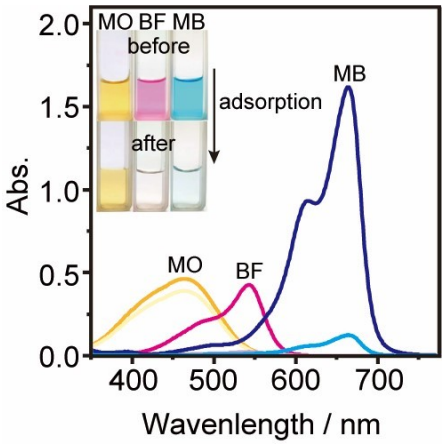

Fig. S8 The UV-vis absorption spectra of the MO, BF and MB single solution before and after adsorption by MGO@CP5. The insert is the photographic pictures of MO, BF and MB supernatant before and after adsorption on MGO@CP5.

Table S1 Nitrogen adsorption-desorption parameters of MGO@CP5

Adsorbent	S_{BET} / m^2 g^{-1}	V / m^3 g^{-1}	D_P / nm
MGO@CP5	128.3	0.35	4.03

Table S2 The data of adsorption kinetics of MGO@CP5 towards BF and MB

Organic dyes		BF	MB
Pseudo first-order model	k_1 (min^{-1})	0.1646	0.1868
	R^2	0.7146	0.8638
Pseudo second-order model	k_2 (g mg^{-1} min^{-1})	0.6277	0.3016
	R^2	0.9998	0.9998
Elovich model	β (g mg^{-1})	1.8167	1.0389
	k_2 (g mg^{-1} min^{-1})	66625	1620.1
	R^2	0.9065	0.9447
Intraparticle diffusion model	k_p (mg g^{-1} $min^{-0.5}$)	8.6552	9.1908
	R^2	0.9490	0.9854
	k_p (mg g^{-1} $min^{-0.5}$)	3.788	4.462
	R^2	/	/
	k_p (mg g^{-1} $min^{-0.5}$)	0.5517	1.1290
	R^2	0.9334	0.9762
	k_p (mg g^{-1} $min^{-0.5}$)	0.1971	0.3534
	R^2	0.9184	0.8587

Table S3 The data of adsorption isotherm of MGO@CP5 towards BF and MB

Isotherm model		BF	MB
Langmuir model	q_m (mg g^{-1})	132.10	239.23
	K_L (L mg^{-1})	0.3314	0.0383
	R^2	0.9911	0.9942
Freundlich model	K_F (mg g^{-1} (L $mg^{-1})^{1/n}$)	46.125	16.061
	n	4.1387	1.6172
	R^2	0.9876	0.9807
Temkin model	K_T (mg L^{-1})	52.867	0.4843
	a	14.218	47.776
	R^2	0.9094	0.9699

Table S4 Comparison of adsorption capacities towards MB and BF with various adsorbents

Adsorbent	Adsorption capacity of adsorbate (mg g^{-1})		Reference
	MB	BF	
Activated carbon fibers	21.3	—	1
PVA-supported GO aerogels	~25	—	2
$MnFe_2O_4$	25.78	—	3
Algae@Fe_3O_4	48.41	—	4
Fe_3O_4-clicked GO	109.5	—	5
Fe_3O_4-MNPs-AC	78.76	—	6
3D-MGFs	298	—	7
CP5-MNPs	136.29	—	8
3D-MSNG-1	171.53	—	9
Snowflake-shaped magnetic micro-/nanostructure	142.9	—	10
Fe_3O_4-CD	—	21.91	11
β-CDP-COOH	—	70	12
Hyd/CB	—	33.75	13
XGACCF	—	63.35	14
Agar-GO	79.51	38.11	15
XG/CFLO	24.54	36.23	16
Fe_3O_4@GO@PDA@poly(NASS-co-DMC)	170.3	289.7	17
MGO@CP5	240	132.1	This work

Reference

1 L. Zhang, L. Y. Tu, Y. Liang, Q. Chen, Z. S. Li, C. H. Li, Z. H. Wang and W. Li, *RSC Adv.*, 2018, **8,** 42280-42291.

2 J. Dai, T. Huang, S. Q. Tian, Y. J. Xiao, J. H. Yang, N. Zhang, Y. Wang and Z. W. Zhou, *Mater. Des.*, 2016, **107,** 187-197.

3 L. Yang, Y. Zhang, X. Liu, X. Jiang, Z. Zhang, T. Zhang and L. Zhang, *Chem. Eng. J.*, 2014, **246,** 88-96.

4 P. Pietrzyk, E. I. Borowska, P. Hejduk, B. C. Camargo, M. Warczak, T. P. Nguyen, A. Pregowska, M. Gniadek, J. Szczytko, S. Wilczewski and M. Osial, *Environ. Sci. Pollut. Res.*, 2023, **30,** 62689-62703.

5 M. Namvari and H. Namazi, *Int. J.Environ. Sci. Technol.*, 2014, **11,** 1527-1536.

6 A. R. Bagheri, M. Ghaedi, A. Asfaram, A. A. Bazrafshan and R. Jannesar, *Ultrason. Sonochem.*, 2017, **34,** 294-304.

7 Y. Yang, G. Hu, F. Chen, J. Liu, W. Liu, H. Zhang and B. Wang, *Chem. Comm.*, 2015, **51,** 14405-14408.

8 H. Zhang, J. R. Wu, X. Wang, X. S. Li, M. X. Wu, F. Liang and Y. W. Yang, *Dyes Pigm.*, 2019, **162,** 512-516.

9 Y. Rong, Y. Huang, P. Jin, C. Yang, Z. Zhong, C. Dong and W. Liang, *J. Water Process. Eng.*, 2020, **37,** 101345-101356.

10 X. M. Zhang, J. Y. Liu, S. J. Kelly, X. J. Huang and J. H. Liu, *J. Mater. Chem. A*, 2014, **2,** 11759-11768.

11 J. H. Ning, D. E. Chen, Y. L. Liu, S. E. Huang, F. X. Wang, R. Wei, Q. C. Hu, J. Q. Wei and C. Sun, *J. Cent. South Univ.*, 2022, **28,** 3666-3680.

12 H. Pu, P. Tang, L. Zhao, Q. Sun, Y. Zhai, Z. Li, N. Gan, Y. Liu, X. Ren and H. Li, *RSC Adv.*, 2020, **10,** 20905-20914.

13 P. M. Pakdel, S. J. Peighambardoust, R. Foroutan, N. Arsalani and H. Aghdasinia, *Int. J. Biol. Macromol.*, 2022, **222**, 2083-2097.

14 I. Spiridon, I. Apostol, N. C. Anghel and M. F. Zaltariov, *Appl. Organomet. Chem.*, 2022, **36,** e6670-e6686.

15 C. M. B. D. Araujo, M. G. Ghislandi, A. G. Rios, G. R. B. D. Costa, B. F. D. Nascimento, A. F. P. Ferreira, M. A. D. Motta Sobrinho and A. E. Rodrigues, *Colloids Surf. A Physicochem. Eng. Asp.*, 2022, **639,** 128357-128371.

16 I. Apostol, N. Anghel, F. Doroftei, A. Bele and I. Spiridon, *Mater. Today Chem.*, 2023, **27,** 101299-121314.

17 C. Bo, Z. Jia, B. Liu, X. Dai, G. Ma and Y. Li, *J. Taiwan Inst. Chem. Eng.*, 2022, **138,** 104499-104511.